Characterization of InN layers grown by high-pressure chemical vapor deposition

M. Alevli, G. Durkaya, A. Weerasekara, A. G. U. Perera, and N. Dietz[a)]
Department of Physics and Astronomy, Georgia State University, Atlanta, Georgia 30303

W. Fenwick, V. Woods, and I. Ferguson
School of Electrical and Computer Engineering, Georgia Institute of Technology, Atlanta, Georgia 30332

(Received 4 May 2006; accepted 21 July 2006; published online 13 September 2006)

Structural and optical properties of indium nitride (InN) layers grown by high-pressure chemical vapor deposition (HPCVD) on sapphire and GaN epilayers have been studied. HPCVD extends processing parameters beyond those accessible by molecular beam epitaxy and metal organic chemical vapor deposition, enabling the growth of epitaxial InN layers at temperatures as high as 1150 K for reactor pressures around 15 bars, leading to vastly improved material properties. InN layers grown on GaN(0002) epilayers exhibit single-phase InN(0002) x-ray diffraction peaks with full width at half maximum (FWHM) around 430 arc sec. Optical characterization of the InN layers by infrared (IR) reflectance reveals free carrier concentrations in the low to mid-10^{+19}-cm^{-3} and optical dielectric function $\varepsilon_\infty=5.8$. The optical properties in the visible and near IR spectral ranges were analyzed by transmission spectroscopy, showing an absorption edge around 1.5 eV. The shift of the absorption edge correlates with deviations in the InN stoichiometry, indicating that the understanding and control of the point defect chemistry of InN is critical for improved material properties. © *2006 American Institute of Physics*. [DOI: 10.1063/1.2352797]

In recent years, research on InN material optimization has dramatically increased, largely due to the crucial importance of indium-rich group III-nitride alloys in novel device structures for solid-state lighting, photovoltaics, spintronics, or terahertz applications utilizing the large spectral tunability and multifunctionality of group III-nitride alloys. However, the integration of indium-rich group III-nitride layers into $Ga_{1-x}Al_xN$ alloys strongly depends on the *existence of overlapping processing windows* as well as the precise control of the thermal decomposition pressures and stoichiometry of indium-rich alloys at the optimum processing temperatures.

Presently, the most efficient growth of wide band gap group III-nitride semiconductors are achieved by metal organic chemical vapor deposition (MOCVD) and molecular beam epitaxy (MBE). However, the epitaxial growth of InN under low-pressure conditions such as MOCVD or MBE is problematic due to large thermal decomposition pressure at the optimum growth temperature, creating conflicting material properties due to point defect chemistry in InN, which at present is not well understood.[1,2] Surface stabilization data have shown that InN can be grown at much higher temperatures if stabilized at high nitrogen pressures,[3] evoking the development of a novel high-pressure chemical vapor deposition (HPCVD) system at Georgia State University. This approach allows us to control the vastly different partial pressures of the constituents involved in the growth of indium-rich group III-nitride alloys.[4–9] The combination of HPCVD and real-time process monitoring/control has been demonstrated to be a viable method to improve the InN material properties, with InN growth temperatures as high as 1150 K for reactor pressures around 15 bars. This is a major step towards the fabrication of indium-rich group III-nitride heterostructures by providing a closer match to the processing windows used for GaN–AlN alloys.

The InN layers have been grown by HPCVD, a high-pressure flow channel reactor with incorporated real-time optical characterization capabilities in order to study and optimize InN nucleation and growth. Ammonia (NH_3) and trimethyl indium (TMI) are employed as precursors in a pulsed injection scheme utilizing pulse width, precursor pulse separation, and cycle sequence time as control parameters in order to control the gas phase and surface chemistry kinetics. The precursors are embedded in a high-pressure carrier gas stream and injected in the reactor utilizing a temporally controlled gas injection system. This approach enables the precise control/suppression of gas phase reactions and the tailoring of surface chemistry processes, which are monitored in real time by UV absorption spectroscopy and principal angle reflectance spectroscopy.

The InN layers investigated here have been grown at temperatures around 1150 K, a reactor pressure of 15 bars, an ammonia to TMI precursor ratio of 600, and total gas flows between 12 and 15 slm (standard liters per minute). During the growth, the gas flow as well as the reactor pressure are maintained constant at all times. The temperature setting refers to the calibrated correlation of the analyzed blackbody radiation as a function of the power setting of the substrate heaters and is not corrected for the change in surface emissivity during the growth. Details of the HPCVD reactor, the growth configuration, as well as real-time optical characterization techniques employed have been published elsewhere.[4,6–9]

The x-ray diffraction (XRD) measurements have been carried out in a $\theta-2\theta$ coupled geometry using Cu $K\alpha$ x rays to evaluate the presence of secondary phases or polycrystallinity. A 1/2 deg slit is used on the incident beam optics and a 1/4 deg slit on the diffracted beam optics for XRD. The Raman spectra are observed in the backscattering configuration. All Raman spectra are normalized to the peak intensity of the E_2(high) phonon feature. Room temperature IR reflection measurements have been performed over the frequency

[a)]Author to whom correspondence should be addressed; electronic mail: ndietz@gsu.edu

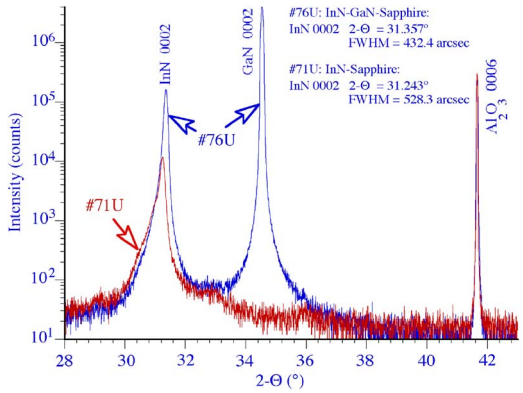

FIG. 1. (Color online) XRD spectra for InN layers grown on sapphire substrate (71U) and virtual GaN/sapphire substrate (76U).

range of 200–8000 cm^{-1} (50–1.25 μm) by using a Perkin-Elmer system 2000 fast Fourier transformed infrared spectrometer and Graesby optical reflection accessory setup. All IR reflection spectra were taken under near normal (~8 deg) incident light arrangement in order to minimize anisotropy effects. Room temperature transmission measurements were performed with a custom build near-infrared–visible–UV spectrometer, which consists of a triple-grating 1/2 m monochromator with phase-sensitive signal detection and processing. A photomultiplier and InGaSb or CdMnTe photodiodes are utilized as detectors for the appropriate wavelength regions.

Figure 1 shows the variation of XRD patterns on a logarithmic scale for InN layers grown directly on sapphire and GaN epilayers/sapphire substrates. The XRD peaks for samples 76U and 71U are centered at $2-\theta=31.357$ and 31.243 deg, respectively. These peaks correspond to the diffraction of the hexagonal phase InN(0002) plane. The full width at half maximum (FWHM) of InN(0002) peaks are 432 and 528 arc sec for the InN layers deposited on GaN/sapphire and sapphire substrates, respectively. The slight asymmetry on the left hand of the InN(0002) peaks may indicate the presence of a second phase in very close proximity, which will need further studies to clarify the origin.

Figure 2 shows Raman spectra of InN samples grown on sapphire substrate (71U) and GaN/sapphire substrate (76UL), which were analyzed using excitation energy of 2.33 eV. The two optical phonon modes of hexagonal InN at 300 K analyzed in Raman spectra are E_2(high) and A_1(LO). The peak centered at wave numbers in the range of

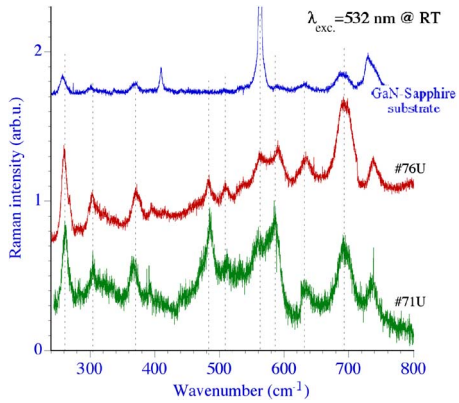

FIG. 2. (Color online) Raman spectra for InN layers grown on sapphire substrate (71U) and on a GaN epilayer (76U).

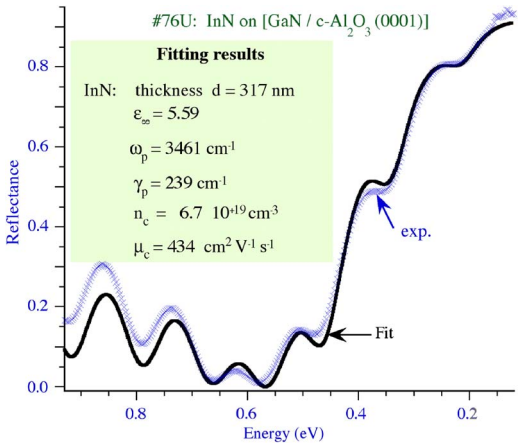

FIG. 3. (Color online) IR reflectance spectrum and best fit for an InN layer deposited on a virtual GaN/sapphire substrate (76U).

489–492 cm^{-1} is attributed to the scattering of light from E_2(high) phonon mode which is most sensitive to strain,[10] whereas the peak at 587 cm^{-1} is assigned to A_1(LO) phonons in InN. The peak positions are in good agreement with those found in InN layers grown by MBE and MOCVD.[1] Based on the allowed phonon mode peak positions for E_2(high) and A_1(LO), our experimental peak positions are similar to the calculated values of 483 and 588 cm^{-1} by Davydov and Klochikhin.[1]

Figure 3 depicts the IR reflectance spectrum for sample 76U and the analysis of optical properties in the IR region. The dielectric functions of the InN and GaN layers are modeled using Eq. (1) assuming two contributions, one of a Lorentz oscillator for phonons and the second one is the classical Drude model for the plasma permittivity,[11,12]

$$\varepsilon(\omega)=\varepsilon_\infty\left[1+\frac{\omega_{\mathrm{LO}}^2-\omega_{\mathrm{TO}}^2}{\omega_{\mathrm{TO}}^2-\omega^2-i\omega\Gamma}+\frac{\omega_P^2}{\omega^2+i\omega\gamma_P}\right], \tag{1}$$

where ε_∞ is the high frequency dielectric constant, ω_{LO} and ω_{TO} are LO and TO frequencies of E_1 phonon mode, ω_P is the plasma frequency, and Γ and γ_P are the two corresponding damping constants. Similarly, the dielectric functions for the GaN epilayer and sapphire substrate are modeled as described in Ref. 12. A matrix method[13] is used to calculate the multilayer stack reflection. The optical properties of the GaN layer were measured and analyzed using a three-layer reflection model (air/GaN/sapphire) before the InN layer was deposited. The best fit parameters for the GaN film was obtained using the nonlinear Levenberg-Marquardt fitting algorithm.[14] Thereafter, the IR reflection of InN/GaN/sapphire structure has been measured and the best fit parameters for InN film have been obtained by using the same fitting algorithm as above. The frequencies of the LO and TO phonon modes were kept constant at 593 and 576 cm^{-1} during the fitting process. The free carrier concentrations were calculated by

$$n_c=\frac{\omega_P^2 m_{\mathrm{eff}}\varepsilon_\infty\varepsilon_0}{q^2}, \tag{2}$$

with ω_P obtained from the fitting process. In Eq. (2), m_{eff} is the effective mass of electron in InN, ε_0 is permittivity in vacuum, and q is the electron charge. The electron effective mass was set as $0.09m_0$,[15] where m_0 is the free electron mass. The change of the electron effective mass as a function of the

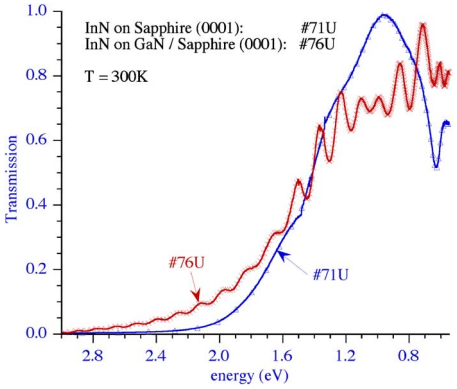

FIG. 4. (Color online) Transmission spectra for InN grown on sapphire substrate (71U) and GaN epilayer/sapphire substrate (76U).

free carrier concentration is not taken into account. The average of the values ε_∞ obtained from the fittings is 5.59 and is used for the free carrier calculation.

The best fit approximation of the experimental data shown in Fig. 3 reveals an InN layer thickness $d=317$ nm, a plasma frequency $\omega_P=3461$ cm^{-1}, and a plasma damping constant $\gamma_P=239$ cm^{-1}. The carrier mobility μ_c is calculated via the effective mass and the damping constant[16] γ_P and found to be $\mu_c=434$ cm^{-2} V^{-1} s^{-1}.

Figure 4 shows the room temperature transmission spectra for samples 71U and 76U, taken at the same spots as the XRD spectra shown in Fig. 1 were taken. Each spectrum is corrected for the substrate and spectrometer response characteristics. The calculated absorption spectra indicate an absorption edge around 1.5 eV with absorption structures around 1.2 and 0.7 eV. Sample 76U exhibits characteristic interference fringes due to the underlying GaN epilayer of 1789 nm thickness. The optical analysis on InN layers grown under similar conditions but with slight variations in the ammonia:TMI flow ratio (NH_3:TMI=600±30) showed that these small deviations in the InN stoichiometry shift the absorption edge from 1.5 down to 1.1 eV, while the free carrier concentration and mobility values obtained by IR reflectance are almost unchanged. The XRD analysis showed single-phase InN(0002) peaks with a slight broadening to FWHM values for ammonia:TMI flow ratios below 570.

The correlation of absorption edge shift and free carrier concentration as obtained by IR reflectance does not support the proposed Moss-Burstein effect[17] as the leading cause for the shift of the fundamental absorption edge to higher values when the carrier concentration is increased. Additional effects such as stoichiometry deviations[18] and the associated point defect chemistry have to be considered to understand the physical properties of InN.

As shown previously,[7–9] ammonia:TMI flow ratios below 500 cause an absorption edge shift down well below 0.7 eV, while the free carrier concentration remains in the mid-10^{+19}-cm^{-3}. For ammonia:TMI flow ratios below 500 the XRD analysis has shown also the presence of the InN(101) phase in addition to the InN(0002) phase.

No equivalent changes are found in the Raman spectra that would provide a link between the appearance of the InN(101) peak in the XRD spectra and changes in the E_2(high) and A_1(LO) Raman modes. The analysis of the E_2(high) and A_1(LO) Raman modes as a function of the ammonia:TMI flow ratio also provided no direct correlation between free carrier concentration and InN stoichiometry deviations for the InN layers investigated. Further studies on InN layers grown in an expanded process window are needed to correlate the point defect chemistry, growth temperature, and reactor pressure with the structural and optical properties of InN.

In conclusion we have studied the structural and optical properties of InN layers grown by HPCVD on quasi-lattice-matched GaN epilayer/sapphire substrates and sapphire substrates. The XRD analysis showed high-quality, single-phase InN(0002) peaks with hexagonal symmetry and a FWHM around 430 arc sec for InN layers deposited on GaN epilayers. The FWHM increases with the lattice mismatch to about 530 arc sec for InN deposited on sapphire substrates. Sharp E_2(high) and A_1(LO) at 488 and 590 cm^{-1} phonon modes are observed. At present, the free carrier concentrations in these InN layers are in the mid-10^{+19}-cm^{-3} and carrier mobilities around 430 cm^{-2} V^{-1} s^{-1}, values that can be improved upon further process optimization. The transmission spectra indicate that the band gap of the InN layers grown by HPCVD is well above 1 eV, which is contrary to results reported for plasma-assisted MBE grown InN layers. Our results also indicate that the observed absorption edge shift does not follow the Moss-Burstein effect but is extremely sensitive to small deviations in the InN stoichiometry, requiring a precise control of gas phase and surface chemistry processes.

This work was supported by NASA Grant No. NAG8-1686 and GSU-RPE.

[1] V. Yu. Davydov and A. A. Klochikhin, Semiconductors **38**, 861 (2004).
[2] K. S. A. Butcher and T. L. Tansley, Superlattices Microstruct. **38**, 1 (2005).
[3] J. MacChesney, P. M. Bridenbaugh, and P. B. O'Connor, Mater. Res. Bull. **5**, 783 (1970).
[4] N. Dietz, M. Strassburg, and V. Woods, J. Vac. Sci. Technol. A **23**, 1221 (2005).
[5] N. Dietz, M. Alevli, H. Kang, M. Straßburg, V. Woods, I. T. Ferguson, C. E. Moore, and B. H. Cardelino, Proc. SPIE **5912**, 78 (2005).
[6] B. H. Cardelino, C. E. Moore, C. A. Cardelino, and N. Dietz, Proc. SPIE **5912**, 86 (2005).
[7] N. Dietz, M. Alevli, V. Woods, M. Strassburg, H. Kang, and I. T. Ferguson, Phys. Status Solidi B **242**, 2985 (2005).
[8] N. Dietz, in *III-Nitrides Semiconductor Materials*, edited by Z. C. Feng (Imperial College Press, 2006), Chap. 6, pp. 203–235.
[9] V. Woods and N. Dietz, Mater. Sci. Eng., B **127**, 239 (2006).
[10] V. Y. Davydov, V. V. Emtsev, I. N. Goncharuk, A. N. Smirnov, V. D. Petrikov, V. V. Mamutin, V. A. Vekshin, S. V. Ivanov, M. B. Smirnov, and T. Inushima, Appl. Phys. Lett. **75**, 3297 (1999).
[11] J. S. Thakur, G. W. Auner, D. B. Haddad, R. Naik, and V. M. Naik, J. Appl. Phys. **95**, 4795 (2004).
[12] Z. G. Hu, M. Strassburg, A. Weerasekara, N. Dietz, A. G. U. Perera, M. H. Kane, A. Asghar, and I. T. Ferguson, Appl. Phys. Lett. **88**, 061914 (2006).
[13] C. C. Katsidis and D. I. Siapkas, Appl. Opt. **41**, 3978 (2002).
[14] *Numerical Recipes in C: The Art of Scientific Computing*, edited by W. H. Press, S. A. Teukolsky, W. T. Vetterling, and B. P. Flannery, 2nd ed. (Cambridge University Press, Cambridge, MA, 1992), p. 681.
[15] T. Inushima, M. Higashiwaki, and T. Matsui, Phys. Rev. B **68**, 235204 (2003).
[16] A. Kasic, M. Schubert, Y. Saito, Y. Nanishi, and G. Wagner, Phys. Rev. B **65**, 115206 (2002).
[17] W. Walukiewicz, S. X. Li, J. Wu, K. M. Yu, J. W. Ager III, E. E. Haller, H. Lu, and W. J. Schaff, J. Cryst. Growth **269**, 119 (2004).
[18] P. P.-T. Chen, K. S. A. Butcher, M. Wintrebert-Fouquet, R. Wuhrer, M. R. Phillips, K. E. Prince, H. Timmers, S. K. Shrestha, and B. F. Usher, J. Cryst. Growth **288**, 241 (2006).